




# CD19<sup>+</sup> tumor-infiltrating B-cells prime CD4<sup>+</sup> T-cell immunity and predict platinum-based chemotherapy efficacy in muscle-invasive bladder cancer

Qi Jiang<sup>1</sup> · Qiang Fu<sup>2</sup> · Yuan Chang<sup>3,4</sup> · Zheng Liu<sup>3,4</sup> · Junyu Zhang<sup>3,4</sup> · Le Xu<sup>5</sup> · Yu Zhu<sup>3,4</sup> · Yiwei Wang<sup>6</sup> · Weijuan Zhang<sup>1</sup> · Jiejie Xu<sup>2</sup> 

Received: 18 January 2018 / Accepted: 20 September 2018 / Published online: 26 September 2018  
© Springer-Verlag GmbH Germany, part of Springer Nature 2018

## Abstract

**Purpose** CD19<sup>+</sup> tumor-infiltrating B-cells (CD19<sup>+</sup> TIB) play a crucial role in tumorigenesis, but their clinical relevance in muscle-invasive bladder cancer (MIBC) remains unknown. This study aimed to investigate the prognostic value of CD19<sup>+</sup> TIB for post-surgery survival and adjuvant chemotherapy response in MIBC.

**Experimental design** We assessed TIB by immunohistochemical staining of CD19 in 246 MIBC patients from Zhongshan Hospital and Shanghai Cancer Center. We evaluated the survival benefit of platinum-based chemotherapy according to CD19<sup>+</sup> TIB. The mechanism underlying CD19<sup>+</sup> TIB antitumor immunity was explored through the Cancer Genome Atlas (TCGA) dataset analysis and an in vitro Ag presentation assay.

**Results** CD19<sup>+</sup> TIB extensively infiltrated into the tumor stroma of MIBC. Adjuvant chemotherapy (ACT) led to a significantly increased benefit in the high CD19<sup>+</sup> TIB MIBC patients ( $P=0.003$ ). In multivariate analysis, high CD19<sup>+</sup> TIB MIBC patients had significantly longer OS with ACT in the discovery set (HR = 0.487,  $P=0.038$ ). TCGA gene expression analyses showed enrichment of adaptive immunity, T-cell-mediated immunity, and antigen-presentation signaling pathways in high CD19<sup>+</sup> TIB MIBC patients. Moreover, CD19<sup>+</sup> TIB co-localized with activated CD4<sup>+</sup> TIT and expressed surface markers characteristic of antigen-presenting cells. Finally, an antigen-presentation assay demonstrated the antigen-presentation function of CD19<sup>+</sup> TIB.

**Conclusion** CD19<sup>+</sup> TIB was identified as an independent prognostic factor, which could predict for post-surgery survival and platinum-based ACT benefits in MIBC. CD19<sup>+</sup> TIB serve as antigen-presenting cells (APCs) to activate CD4<sup>+</sup> TIT in the tumor environment of MIBC.

**Keywords** CD19<sup>+</sup> TIB · Muscle-invasive bladder cancer · Adjuvant chemotherapy · Antitumor response

Qi Jiang, Qiang Fu and Yuan Chang contributed equally to this work.

**Electronic supplementary material** The online version of this article (<https://doi.org/10.1007/s00262-018-2250-9>) contains supplementary material, which is available to authorized users.

✉ Weijuan Zhang  
weijuanzhang@fudan.edu.cn

✉ Jiejie Xu  
jjxufdu@fudan.edu.cn

<sup>1</sup> Department of Immunology, School of Basic Medical Sciences, Fudan University, Building 13, No. 130, Dongan Road, Shanghai 200032, China

<sup>2</sup> Department of Biochemistry and Molecular Biology, School of Basic Medical Sciences, Fudan University, Building 7, No. 130, Dongan Road, Shanghai 200032, China

## Abbreviations

ACT	Adjuvant chemotherapy
CD19 <sup>+</sup> TIB	CD19 <sup>+</sup> tumor-infiltrating B-cell(s)
GSEA	Gene set enrichment analysis
MIBC	Muscle-invasive bladder cancer

<sup>3</sup> Department of Urology, Fudan University Shanghai Cancer Center, Shanghai, China

<sup>4</sup> Department of Oncology, Shanghai Medical College, Fudan University, Shanghai, China

<sup>5</sup> Department of Urology, Ruijin Hospital, School of Medicine, Shanghai Jiao Tong University, Shanghai, China

<sup>6</sup> Department of Urology, Ninth People's Hospital, School of Medicine, Shanghai Jiaotong University, Shanghai, China

RC	Radical cystectomy
TCGA	The Cancer Genome Atlas
TIT	Tumor-infiltrating T-cell(s)
TMA	Tissue microarray

## Introduction

As the most common malignant tumor of the urinary system, bladder cancer accounts for 4%–5% of all new cancer diagnoses in adults [1]. The major pathological type of bladder cancer is transitional cell carcinoma, which is classified into nonmuscle-invasive bladder cancer and muscle-invasive bladder cancer (MIBC) according to the depth of tumor invasion [2]. For MIBC and high-risk NMIBC, radical cystectomy (RC) is recommended as the primary treatment, but follow-up has shown that approximately 50% of patients experience relapse or metastases [3]. Hence, additional chemotherapy is applied to improve the outcome of MIBC patients after RC [4]. However, only a fraction of patients experience a clinical response and survival benefit from adjuvant chemotherapy (ACT), leading to an urgent need to develop efficient predictive indicators to identify these MIBC patients. Currently, the common prognostic predictors, such as the tumor node metastasis (TNM) staging system and molecular markers, have been widely used for risk assessments and treatment strategies by clinicians. However, most of the prognostic indicators lack robust predictive accuracy because of the high heterogeneity between patients or pathological subtypes. Recently, tumor stromal immune compartments have been found to affect disease progression and to be associated with the survival of patients [5, 6].

B-cells participate in the human adaptive immune system by differentiating into plasma cells and producing antibodies in response to a pathogen [7]. Additionally, B-cells operate as effective antigen-presenting cells (APCs) to prime antigen-specific CD4<sup>+</sup>T-cells or secrete cytokines and chemokines to recruit and activate other immune cells in the tumor microenvironment [8]. However, previous studies have suggested that the B-cell lineage could participate in carcinogenesis and tumor progression, leading to controversy about B-cell roles in some solid tumors [9, 10]. Pylayeva-Gupta et al. found that CD19<sup>+</sup>CD1d<sup>hi</sup>CD5<sup>+</sup> B-cells promote pancreatic tumor progression via producing IL-35 and suppressing antitumor immunity [5]. In addition, pro-inflammatory cytokines, such as IFN- $\gamma$  and TNF- $\alpha$ , were upregulated in B-cell knockout mice compared with naive wild-type mice, suggesting an anti-inflammatory role of B-cells [10, 11]. Conversely, the tumor-specific IgGs produced by plasma cells stimulate high expression of CD86 on antigen-presenting cells and thereby inhibit the progression of human high-grade serous ovarian cancer [12]. However, the role of CD19<sup>+</sup> tumor-infiltrating B-cells (CD19<sup>+</sup>

TIB) in MIBC and the underlying mechanisms remain undetermined.

To elucidate the biological functions and clinical relevance of CD19<sup>+</sup> TIB in MIBC patients, we evaluated CD19<sup>+</sup> TIB quantity in MIBC and investigated its relationship with clinical outcomes, especially in patients treated with ACT. These results may clarify the vital function of CD19<sup>+</sup> TIB in MIBC and provide a possible predictive indicator to aid in ACT decisions for MIBC patients.

## Materials and methods

### Patients and clinical database

This retrospective study enrolled two independent sets of patients. The discovery set included 246 patients from Fudan University Shanghai Cancer Center (Shanghai, China) from 2008 to 2012 and Zhongshan Hospital (Shanghai, China) from 2002 to 2014. Patients with T1 tumors that did not invade the muscular tissue (i.e., NMIBC) were excluded. The clinical and pathological characteristics included age, gender, TNM stage, lymphovascular invasion, tumor size and tumor grade. Tumor size was defined as the longest diameter using an international measurement. All specimens were reappraised via pathologic examinations according to the 2009 TNM classification. The tumor grade was recorded according to the 2004 World Health Organization classification. None of the patients received neoadjuvant chemotherapy before surgery. Patients received four different platinum-based drugs: gemcitabine/carboplatin, gemcitabine/cisplatin, gemcitabine/oxaliplatin or MVAC. Overall survival (OS) was defined as the time from surgery to death from any cause. After surgery, patients were evaluated by physical examination, laboratory studies, and urine cytology every 3 months in the first year, and annually thereafter. The validation set included 427 MIBC patients from the Cancer Genome Atlas (TCGA) database [13], and 57 patients with T1 tumors were excluded. None of these patients received neoadjuvant chemotherapy before surgery.

### Immunohistochemistry and immunofluorescence

The surgical, formalin-fixed and paraffin-embedded specimens were used to construct a tissue microarray (TMA). Immunohistochemistry was performed according to a previously applied protocol [14]. A mouse monoclonal antibody against human CD19 (Abcam, clone 2E2B6B10, 2.5  $\mu$ g/ml) was used as the primary antibody. Negative control slides were treated with nonspecific IgG2a antibody instead of the primary antibody. The immunohistochemistry results were viewed by Image-Pro plus 6.0 (Media Cybernetics Inc., Bethesda, MD). CD19 positive staining cells were evaluated

in a blinded manner by two urinary pathologists independently. The intensity of CD19<sup>+</sup> TIB was calculated as the mean number of CD19 positive cells from three randomized areas of a single tumor. We dichotomized the patients in the discovery set into a high CD19<sup>+</sup> TIB subgroup and low CD19<sup>+</sup> TIB subgroup equally and dichotomized the patients in the validation set into a CD19 mRNA high subgroup and CD19 mRNA low subgroup equally. The TMA was also performed by immunofluorescence described previously [15], and we used anti-CD19 (Abcam, clone 2E2B6B10, 2.5 µg/ml) together with either anti-CD4 (Abcam, clone EPR6855, 0.5 µg/ml) or anti-MHC Class II rabbit mAb (Abcam, clone EPR11226, 2.5 µg/ml). Then, two secondary antibodies, Alexa 594 goat anti-mouse IgG and Alexa 488 goat anti-rabbit IgG were applied. Images were acquired with a Nikon Eclipse Ti-S Microscope.

### Real-time quantitative PCR

Total RNA from fresh human tumor specimens was extracted using TRIzol reagent (Invitrogen) according to the manufacturer's instructions. Real-time quantitative PCR was performed on the Applied Biosystems 7300 Real-Time PCR system using SYBR Green dye (Applied Biosystems) as described by the manufacturer. The primers for CD19 are as follows: 5': CCGGAGAGTCTGACCACCAT and 3': GCACAGCGTTATCTCCCTCT. GAPDH served as an endogenous control. All determinations were performed in triplicate and in at least three independent experiments. The  $\Delta\Delta C_t$  method was applied to estimate relative transcript levels.

### Gene set enrichment analysis (GSEA) and CIBERSORT algorithm

Gene set enrichment analyses of gene expression data were conducted using GSEA [16]. If a gene set had a positive enrichment score, the majority of its members had a higher risk score, and the set was termed "enriched." GSEA was performed to identify the enriched pathway (GO biological process database) in high CD19<sup>+</sup> TIB MIBC patients compared with low CD19<sup>+</sup> TIB MIBC patients via gene expression analysis of 370 samples. Gene sets from Molecular Signatures Database (C5 Gene Ontology signature) of sizes larger than 15 genes were analyzed with 1000 randomized permutations of the patient phenotype. The CIBERSORT algorithm [17], an analytical tool that provides an estimation of the abundances of member cell types in a mixed cell population, was applied to TCGA gene expression database to analyze the associations between the number of B-cells and the level of CD19 mRNA.

### Flow cytometry

We examined the phenotypes of tumor tissue and peripheral blood-derived CD19<sup>+</sup> B-cells, CD4<sup>+</sup> T-cells and MHC II<sup>+</sup> cells from MIBC patients. The cells were stained with the following fluorochrome-conjugated antibodies: Alexa Fluor 488-conjugated anti-CD4 (BD Pharmingen, clone RPA-T4, 1:40), APC-Cy7-conjugated anti-CD3 (BD Pharmingen, clone SK7, 1:40), PE-Cy7-conjugated anti-CD19 (BD Pharmingen, clone SJ25C1, 1:40), PE-Cy7-conjugated anti-CD44 (BD Pharmingen, clone G44-26, 1:40), BV510-conjugated anti-CD80 (BD Pharmingen, clone L307.4, 1:40), BV650-conjugated anti-CD86 (BD Pharmingen, clone 2331, 1:40), APC-conjugated anti-HLA-DR (BD Pharmingen, clone G46-6, 1:40), BV785-conjugated anti-CD11c (BioLegend, clone 3.9, 1:40), and FITC-conjugated anti-CD68 (BD Pharmingen, clone Y1/82A, 1:40). Antibody specificity was tested using matched isotypes. Cells were analyzed by flow cytometry on a FACSCelesta (BD Immunocytometry Systems) according to the manufacturer's instructions, and the data were analyzed with FlowJo software version X (Tree Star). Dead cells were excluded by staining with Fixable Viability Stain 450 (BD Biosciences). All samples were gated on CD45<sup>+</sup> leukocytes based on forward and side scatter plots.

### In vitro Ag presentation assay

Fresh tumor and peripheral blood specimens from four patients with MIBC were obtained immediately after surgery. The tissues were minced and digested in 0.2 U/ml collagenase (Roche) for 3 h. The cell suspension was filtered by 0.45 µm filtration. CD19<sup>+</sup> TIB and peripheral blood B-cells (stained with anti-CD19 antibodies) and CD4<sup>+</sup> tumor-infiltrating T-cells (TIT) (stained with anti-CD4 antibodies) were sorted from cell suspension by flow cytometry. CD4<sup>+</sup> TIT were resuspended in PBS at a concentration of  $2 \times 10^6$ /ml and labeled with 5 µmol/L CFSE for 15 min at 37 °C under constant agitation, then washed and subsequently resuspended in RPMI-1640 (Gibco) supplemented with 10% FBS (Gibco), penicillin, and streptomycin. The human bladder carcinoma cell line TCCSUP (ATCC HTB-5) was purchased from Cell Bank, Chinese Academy of Sciences. TCCSUP cell line lysates were obtained by ultrasonication and filtered by 0.45 µm filtration. CFSE-labeled CD4<sup>+</sup> TIT were cocultured with TCCSUP lysates (ratio 1:1) or with a combination of TCCSUP lysates and CD19<sup>+</sup> TIB/peripheral blood B-cells (ratio 1:1:1), or with a combination of TCCSUP lysates and CD19<sup>+</sup> TIB/peripheral blood B-cells (ratio 1:1:1) and HLA-DR blocking antibodies (BD Biosciences, clone Tu39, 1 µg/ml). In each set, the total number of cells was  $2 \times 10^6$  cells. The dilution of CFSE, CD44 and CD40L (BD Pharmingen,

clone TRAP1, 1:40) by CD4<sup>+</sup> TIT were determined after a 4-day coculture by flow cytometry.

## Statistical analysis

Categorical variables between different groups were analyzed by Chi square or Fisher exact test, and continuous variables between different groups were analyzed by *t* test and Wilcoxon rank-sum test. Kaplan–Meier survival curves and log-rank test were used to test the survival difference between subgroups. Multivariate Cox proportional hazards model containing the categorical CD19<sup>+</sup> TIB variable and other clinical characteristics was applied to obtain statistically significant parameters. All tests were two-sided and were performed at a significance level of 0.05. SPSS 20.0 (SPSS Inc., Chicago, IL) and R software version 3.3.0 were used for the statistical analyses.

## Results

### Immunohistochemistry staining of CD19 and correlation between CD19<sup>+</sup> TIB and prognosis in MIBC patients

To explore the correlation between CD19<sup>+</sup> TIB and the progression of MIBC, we evaluated the presence of CD19<sup>+</sup> TIB by immunohistochemistry in 246 MIBC patients from the discovery set. The staining results of CD19 showed that most CD19<sup>+</sup> TIB were located in the stroma of tumors (Fig. 1a–c) and had a density ranging from 0 to 1000 cells/mm<sup>2</sup>. We analyzed the correlation between CD19<sup>+</sup> TIB and clinicopathologic variables, and there were no significant associations between CD19<sup>+</sup> TIB and clinicopathologic variables, including age, gender, grade, TNM stage and tumor size (Supplementary Table 1). To investigate whether CD19<sup>+</sup> TIB were associated with clinical outcomes, we conducted a Kaplan–Meier analysis. Patients with high CD19<sup>+</sup> TIB had significantly longer survival compared with low CD19<sup>+</sup> TIB patients in the discovery set ( $P=0.003$ ) (Fig. 1d). Furthermore, the multivariate analysis including ACT, TNM stage and CD19<sup>+</sup> TIB also revealed a significant correlation between high CD19<sup>+</sup> TIB and prolonged OS (HR = 0.532; 95% CI = 0.359–0.789), indicating that CD19<sup>+</sup> TIB is an independent prognosticator of MIBC patient survival (Supplementary Table 2).

### Predictive value of CD19<sup>+</sup> TIB with response to adjuvant chemotherapy

After identifying the correlation between CD19<sup>+</sup> TIB and patient survival, we were interested in determining whether CD19<sup>+</sup> TIB had a protective role in ACT efficacy in MIBC.

Therefore, we evaluated the effectiveness of ACT according to CD19<sup>+</sup> TIB frequency. Intriguingly, for MIBC patients with high CD19<sup>+</sup> TIB, adjuvant chemotherapy was a significant protective factor with OS in the discovery set ( $P=0.003$ ), but low CD19<sup>+</sup> TIB patients received no OS benefit from ACT ( $P=0.001$ ) (Fig. 1e, f). In the multivariate analysis for OS in the MIBC patient subgroup with high CD19<sup>+</sup> TIB, the patients who received ACT had significantly longer survival than the patients who did not receive ACT (HR = 0.487; 95% CI = 0.247–0.961;  $P=0.038$ ), but in the low CD19<sup>+</sup> TIB patient subgroup, no significant improvement in OS from ACT was observed (Table 1).

To obtain robust results about the ACT predictive capacity of CD19<sup>+</sup> TIB in MIBC, we developed a TCGA MIBC cohort as a validation set and performed similar survival analyses. First, we analyzed the equivalence of CD19<sup>+</sup> TIB and levels of CD19 mRNA by flow cytometry and RT-PCR in 15 bladder cancers and found a significantly positive correlation between them. Similarly, we computed the number of B-cells in TCGA by the CIBERSORT algorithm and again found a positive correlation between them (Supplementary Fig. 1a, b). Thus, CD19 mRNA expression level was used as a simulation of CD19<sup>+</sup> TIB here. Although no significant OS difference was found between MIBC patients with ACT and patients without ACT in the validation set, regardless of the CD19 mRNA level (Supplementary Fig. 2a, b), the multivariate analyses showed that among the high CD19 MIBC patients, the patients that received ACT had a significantly longer OS compared with those without ACT (HR = 0.366; 95% CI = 0.193–0.694;  $P=0.002$ ) (Supplementary Table 3). Taken together, these results from two clinical MIBC cohorts suggest that MIBC patients with high CD19<sup>+</sup> TIB could receive more OS benefit from post-surgery ACT.

### Functional gene exploration of CD19<sup>+</sup> TIB

To investigate the biological functions of CD19<sup>+</sup> TIB in MIBC, we performed GSEA to explore the gene expression profile of TCGA MIBC patients. We compared the GO biological process gene sets and found that several immune-related signaling pathways, such as lymphocyte migration, regulation of TCR signaling, regulation of antigen receptor-mediated signaling and adaptive immune response, were significantly enriched (NES > 2.2, FDR q-value < 0.001) in CD19 mRNA high patients (Fig. 2a). These results indicated that the presence of CD19<sup>+</sup> TIB was associated with positive regulation of lymphocyte activation in MIBC patients.

Next, we compared the differential gene expression between patients with high CD19 and low CD19 in TCGA MIBC set and found that the expression of genes associated with B-cell activation (BTK, CD79A, CD79B), T-cell activation (IFNG, IL12B, CD86), and antigen presentation

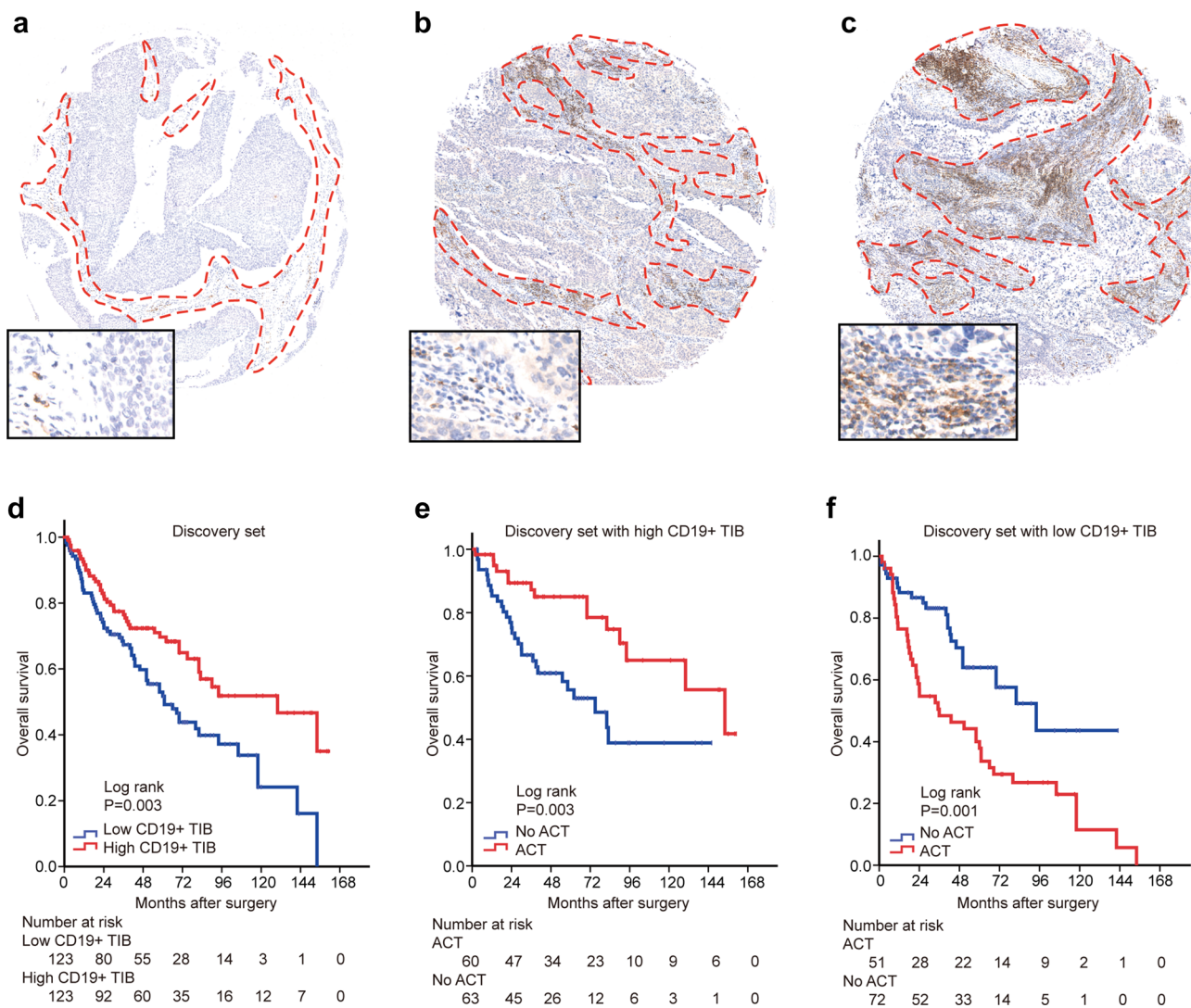


**Fig. 1** Different densities of CD19<sup>+</sup> TIB and their correlation with prognosis or ACT efficacy in MIBC. **a–c** Representative images of **a** low CD19<sup>+</sup> TIB, **b** moderate CD19<sup>+</sup> TIB and **c** high CD19<sup>+</sup> TIB. Dashed lines indicate stromal areas in tumors. **d–f** Kaplan–Meier

analysis for OS of MIBC patients according to different CD19<sup>+</sup> TIB in the discovery set (**d**). Kaplan–Meier analysis for OS of MIBC patients according to ACT in high CD19<sup>+</sup> TIB patients (**e**) and in low CD19<sup>+</sup> TIB patients (**f**)

(HLA-DPB1, HLA-DRB1) were all increased in high CD19 patients (Fig. 2b) [18–20]. These results indicated that high CD19<sup>+</sup> TIB were mostly associated with the initiation of adaptive immunity, especially the antigen-presentation process in MIBC patients.

### Antigen-presentation functions of CD19<sup>+</sup> TIB

Our previous results of functional gene exploration implied that CD19<sup>+</sup> TIB might activate antigen-specific T-cell responses via their antigen-presentation function. To prove this hypothesis, we performed immunohistochemistry and immunofluorescence of CD19, MHC II and CD4 in serial sections of MIBC tumors. Intriguingly,

immunohistochemistry revealed that most CD19<sup>+</sup> TIB were distributed among MHC II<sup>+</sup> cell-rich areas, whereas CD4<sup>+</sup> TIT were located nearby (Fig. 2c). We also found a significant correlation between the density of CD19<sup>+</sup> TIB and MHC II<sup>+</sup> cells or CD4<sup>+</sup> TIT (Fig. 2d, e). Consistently, immunofluorescence showed an expression of MHC II in CD19<sup>+</sup> TIB in the stromal area of tumors while CD19<sup>+</sup> TIB and CD4<sup>+</sup> TIT were directly juxtaposed, supporting cell–cell interactions (Fig. 3a, b). Although MHC II molecules can be expressed by B-cells, DC and macrophages, we found that MHC II<sup>+</sup> CD19<sup>+</sup> cells accounted for approximately 10%–30% of total MHC II<sup>+</sup> cells by flow cytometry, indicating nonnegligible impacts of these CD19<sup>+</sup> TIB on antigen presentation (Supplementary Fig. 3).

**Table 1** Multivariate Cox regression analyses for overall survival in MIBC patients with CD19<sup>+</sup> TIB according to ACT, TNM stage and grade

Characteristic	Overall survival					
	Low CD19 <sup>+</sup> TIB			High CD19 <sup>+</sup> TIB		
	Patients	HR (95% CI)	<i>P</i> value	Patients	HR (95% CI)	<i>P</i> value
Discovery set	123			123		
T classification						
T2	72	1.00 (Reference)		63	1.00 (Reference)	
T3+T4	51	1.500 (0.820–2.745)	0.188	60	1.298 (0.692–2.435)	0.417
N classification						
N0	99	1.00 (Reference)		107	1.00 (Reference)	
N1+N2+N3	24	2.836 (1.405–5.727)	<b>0.004</b>	16	1.132 (0.423–3.025)	0.805
Distant metastasis						
No	102	1.00 (Reference)		102	1.00 (Reference)	
Yes	21	2.110 (1.121–3.969)	<b>0.021</b>	21	3.572 (1.802–7.081)	<b>&lt;0.001</b>
Grade						
Low	21	1.00 (Reference)		14	1.00 (Reference)	
High	102	2.103 (0.936–4.725)	0.072	109	1.159 (0.404–3.323)	0.783
Adjuvant therapy						
No	72	1.00 (Reference)		63	1.00 (Reference)	
Yes	51	1.294 (0.708–2.363)	0.402	60	0.487 (0.247–0.961)	<b>0.038</b>

MIBC muscle-invasive bladder cancer, ACT adjuvant therapy, HR hazard ratio, CI confidence interval  
*P* value < 0.05 marked in bold font shows statistical significance

As it has been reported that CD19<sup>+</sup> TIB can exert antigen-presentation function through MHC II and costimulatory molecules, we detected the expression of costimulatory molecules on CD19<sup>+</sup> TIB by flow cytometry. We found that, compared with CD19<sup>+</sup> peripheral blood B-cells, CD19<sup>+</sup> TIB expressed similar intensities of HLA-DR (Fig. 4c). However, CD19<sup>+</sup> TIB expressed significantly high levels of CD80 and CD86 on their surface compared with CD19<sup>+</sup> peripheral blood B-cells, albeit at moderate levels (Fig. 4a, b). Additionally, CD4<sup>+</sup> TIT expressed high levels of CD44 compared with CD4<sup>+</sup> peripheral blood T-cells (Fig. 4d).

To further illustrate the antigen-presentation function of CD19<sup>+</sup> TIB in MIBC, we performed in vitro antigen-presentation assays. CFSE-labeled CD4<sup>+</sup> TIT were cocultured with TCCSUP cell lysates as a negative control, and then CD19<sup>+</sup> TIB or peripheral blood B-cells were added to test their functions. The proliferation of CD4<sup>+</sup> TIT significantly increased when CD19<sup>+</sup> TIB or peripheral blood B-cells were added to the coculture. Furthermore, the expressions of activation marker CD44 and costimulation marker CD40L on CD4<sup>+</sup> T-cells both increased when CD19<sup>+</sup> TIB or peripheral blood B-cells were added to the coculture. Importantly, the increase in proliferation, CD44 and CD40L expression was all abrogated after the addition of HLA-DR blocking antibodies (Fig. 5). Collectively, these results suggested that CD19<sup>+</sup> TIB activate CD4<sup>+</sup> TIT through an MHC II-mediated antigen-presentation process in MIBC.

## Discussion

Cisplatin-based chemotherapeutic drugs are widely used in a variety of cancers, including ovarian cancer, testicular cancer and bladder cancer [21]. Leow et al. found a positive benefit on OS by cisplatin-based adjuvant chemotherapy in an updated meta-analysis, although this conclusion lacks the support of randomized large sample trials and there are still some patients with poor clinical outcomes and premature metastasis [22]. Thus, it is vitally important to identify convenient and effective predictive indicators to guide the clinical use of adjuvant chemotherapy.

Previous studies have found that different genetic subtypes of bladder cancer have different sensitivities to chemotherapy. For example, research from an MD Anderson MVAC set showed that “P53-like” subtype MIBCs were resistant to neoadjuvant chemotherapy, whereas “basal” subtype MIBCs were chemosensitive. Furthermore, some immune biomarkers, such as FAS ligand (FASLG), CD8B molecule, colony-stimulating factor 1 (CSF-1), and C–C motif chemokine ligand 5 (CCL5), were enriched in basal tumors [23]. However, the association between CD19<sup>+</sup> TIB and clinical outcomes in MIBC remains undetermined.

In this study, we demonstrated the prognostic significance of CD19<sup>+</sup> TIB as an independent predictive parameter for guiding adjuvant chemotherapy. We showed that the MIBC patients who received ACT with high CD19<sup>+</sup> TIB have a longer OS compared to those with low CD19<sup>+</sup>

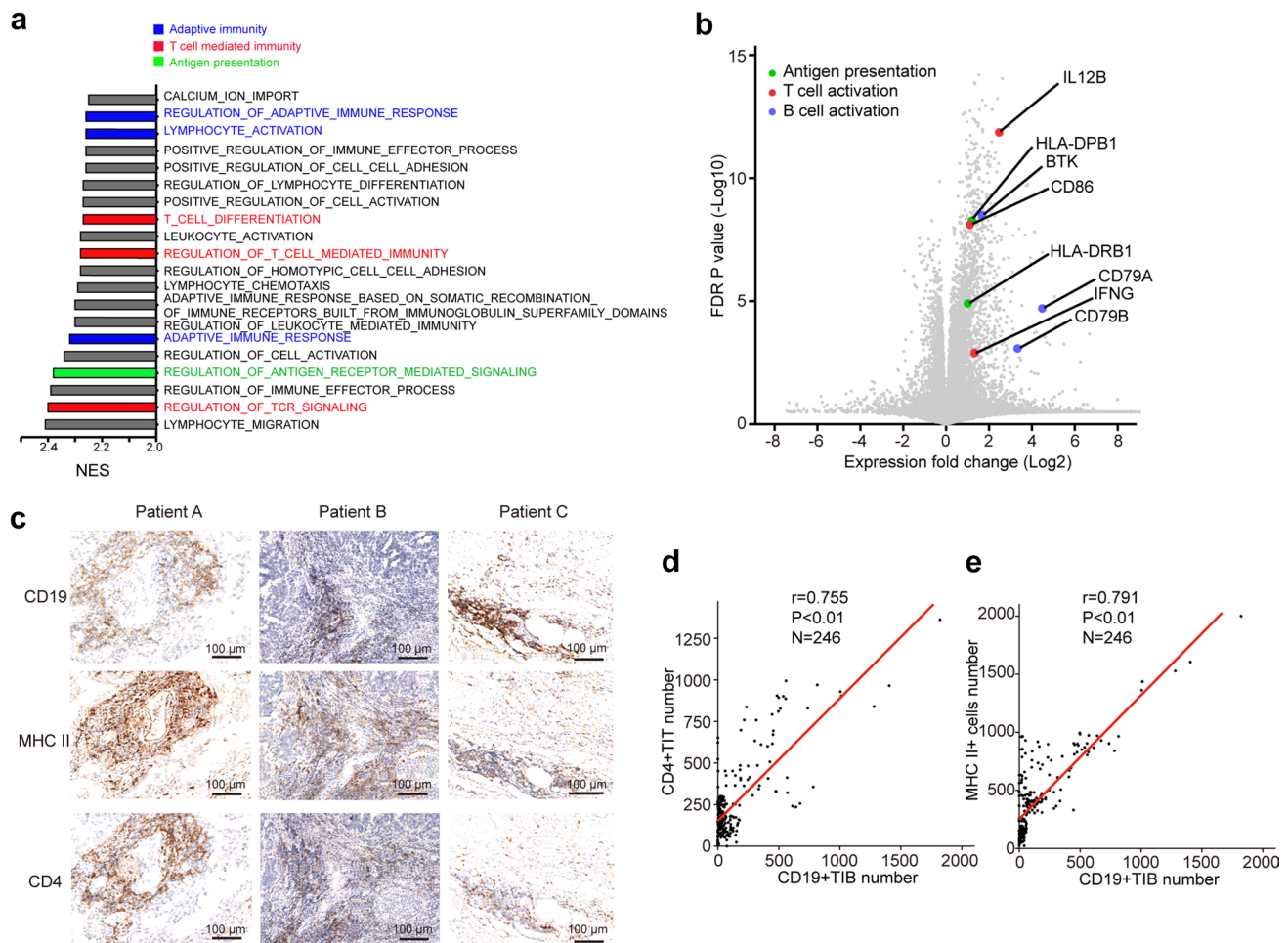


**Fig. 2** Correlation between CD19<sup>+</sup> TIB and molecules related to antigen presentation in specimens and database. **a** The top 20 significant biological pathways and processes in high ( $n=185$ ) vs. low ( $n=185$ ) CD19 MIBC patients. **b** Volcano plot comparing genes in high ( $n=185$ ) vs. low ( $n=185$ ) CD19 MIBC patients. Genes labeled in

blue, red and green represent B-cell activation, T-cell activation and antigen-presentation pathways. **c** Immunohistochemical staining of CD19, MHC II and CD4 on continuous tumor slices of MIBC. Scale bar = 100  $\mu$ m. **d–e** Correlations between the density of CD19<sup>+</sup> TIB and the density of CD4<sup>+</sup> TIT or MHC II<sup>+</sup> cells in the tumors

TIB, indicating that CD19<sup>+</sup> TIB could be a vital element for selecting treatment strategies.

To determine the mechanism through which CD19<sup>+</sup> TIB affect MIBC disease progression and therapeutic responses, we observed the biological characteristics of B-cells under the pathological conditions of tumors. Generally, B-cells participate in the humoral immune response in a variety of diseases (infections, cancers) by differentiating into plasma cells that secrete antigen-specific antibodies to neutralize pathogens [7]. However, B-cells can also deliver influential immune responses directly in certain disease microenvironments. Compelling evidence has demonstrated that increased amounts of intratumoral B-cells are associated with clinical outcome and response to chemotherapy [24]. Jie-Yi Shi et al found that margin-infiltrating B-cells (MIL-B) were a favorable prognostic factor for patients with hepatocellular carcinoma, and MIL-Bs showed an atypical phenotype

(IgD<sup>-</sup>IgG<sup>+</sup>CD27<sup>-</sup>CD38<sup>-</sup>), secreting IFN- $\gamma$ , interleukin 12p40 (IL-12p40), granzyme B, and TRAIL, acting as APCs and activating Th1 cells in the tumor microenvironment [25]. Consistently, B16 melanoma tumor volume and lung metastasis were increased in B-cell-depleted mice. Moreover, B-cell depletion impaired both IFN- $\gamma$  and TNF- $\alpha$  induction by CD4<sup>+</sup> T-cells and CD8<sup>+</sup> T-cells in vivo and also reduced the infiltration of tumor Ag-specific CD8<sup>+</sup> T-cells in vivo [26].

To understand the biological functions of CD19<sup>+</sup> TIB in MIBC and the mechanism underlying ACT therapy efficacy improvement, we analyzed TCGA gene expression data and found that the signaling pathways associated with the adaptive immune response and antigen presentation were enriched in high CD19 MIBC patients. Moreover, the direct contact of CD19<sup>+</sup> MHC II<sup>+</sup> TIB with CD4<sup>+</sup> TIT in human tumor samples, the high expressions of antigen

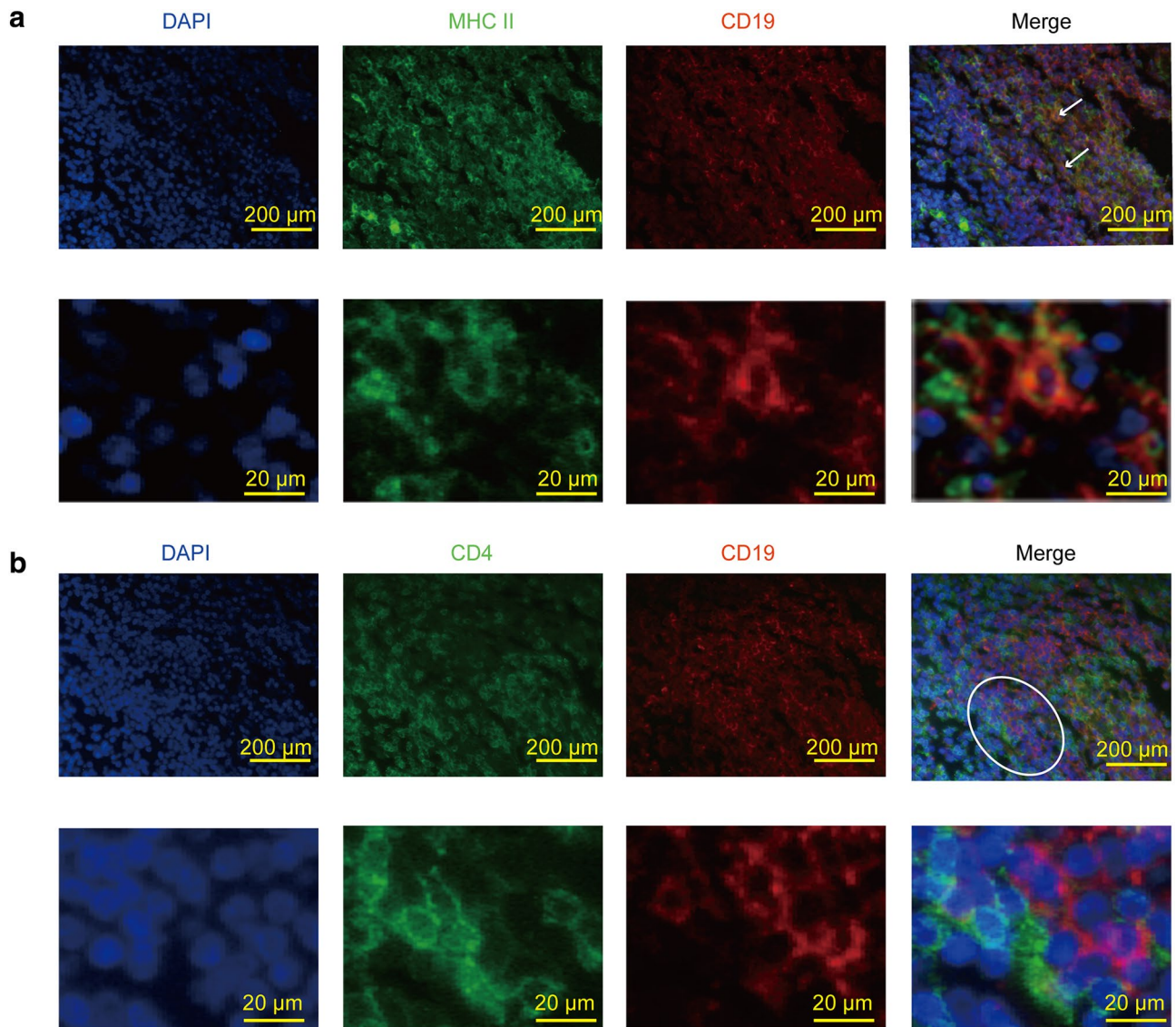


**Fig. 3** Localization of MHC II<sup>+</sup> CD19<sup>+</sup> TIB and CD4<sup>+</sup> TIT in MIBC. **a–b** Immunofluorescence of CD19 (red) and MHC II molecule (green) or CD4 (green) on MIBC tumors. White arrows represent MHC II<sup>+</sup>

CD19<sup>+</sup> TIB. Circled areas represent CD19<sup>+</sup> TIB and CD4<sup>+</sup> TIT that are close to each other. Scale bars = 200 μm or 20 μm

presentation-associated molecular MHC II, CD80 and CD86 on CD19<sup>+</sup> TIB, and the *in vitro* antigen presentation assay all demonstrated that CD19<sup>+</sup> TIB in MIBC could activate CD4<sup>+</sup> TIT in the presence of tumor antigens, which could, in turn, boost the immune cytotoxicity and add to the tumor-killing effects of chemotherapy.

Several studies support our findings. Apetoh et al. showed that chemotherapy drugs lose their therapeutic efficacy in patients with loss-of-function TLR4, which affects the processing and presentation of tumor antigen derived from dying tumor cells [27]. Additionally, Wang et al. found that the patients who had high stromal CD8<sup>+</sup> T-cells are more likely to respond to platinum-based chemotherapy [28].

Thus, our finding that patients with high CD19<sup>+</sup> TIB had prolonged survival may be due to the enhanced priming of effective CD4<sup>+</sup> T-cells by CD19<sup>+</sup> TIB and that patients with low CD19<sup>+</sup> TIB are resistant to platinum-based antitumor chemotherapy may be due to an adaptive immune response reduction and excessive side effects.

To our knowledge, this study is the first to investigate the prognostic associations of CD19<sup>+</sup> TIB and their associations with adaptive immunity and ACT effects in MIBC. However, there are some limitations in this study. First, the clinical investigation in this study is based on retrospective data, which lack unified and standardized platinum-based chemotherapy procedures, and the total numbers of the



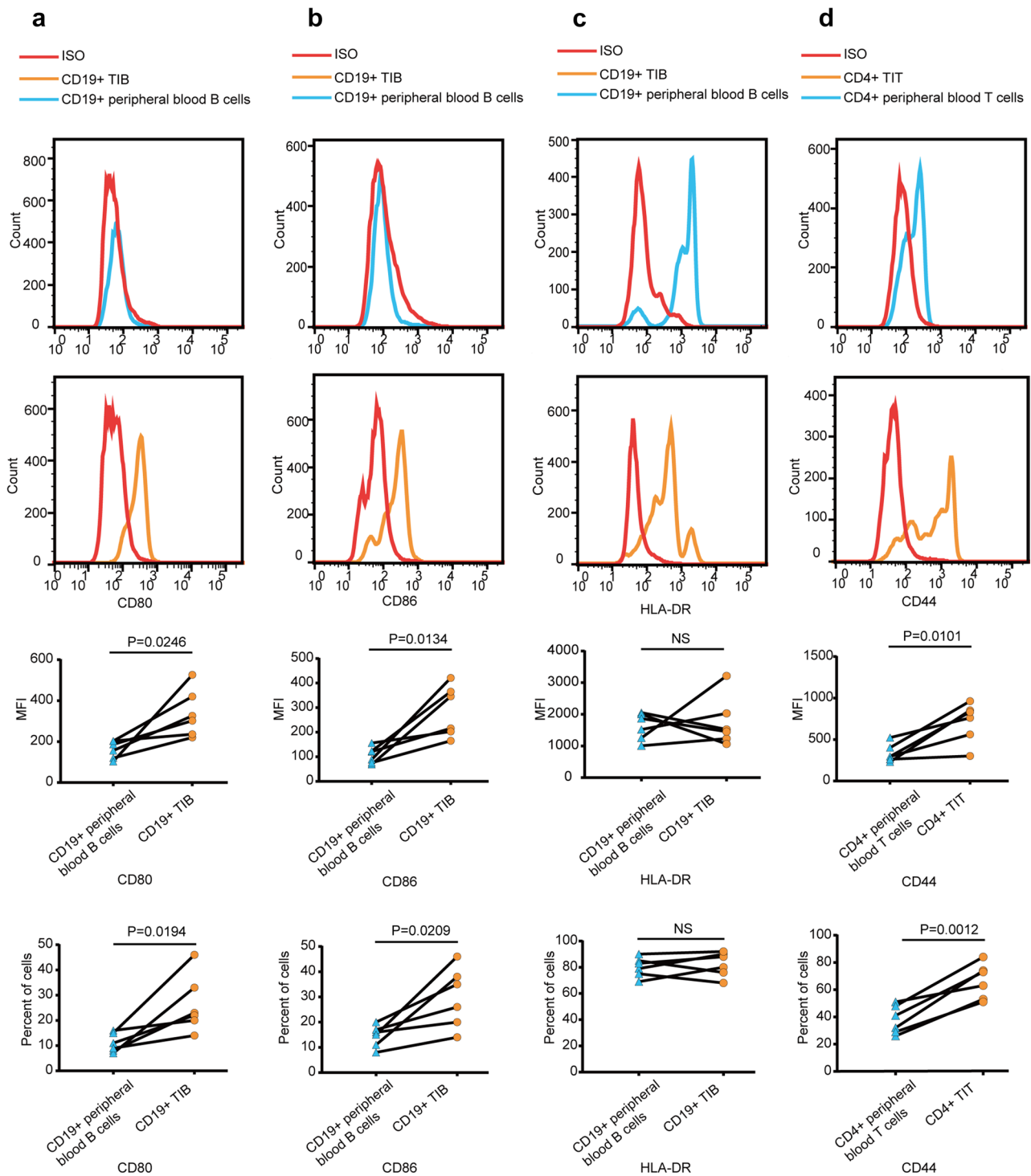


**Fig. 4** Surface phenotype of CD19<sup>+</sup> TIB and CD4<sup>+</sup> TIT in MIBC. **a–c** Representative flow cytometry data showing the expression of CD80, CD86 and HLA-DR on CD19<sup>+</sup> TIB and CD19<sup>+</sup> peripheral blood B-cells. Samples were gated on CD45<sup>+</sup> CD19<sup>+</sup> cells (*n*=6). **d**

Representative flow cytometry data showing expression of CD44 on CD4<sup>+</sup> TIT and CD4<sup>+</sup> peripheral blood T-cells. Samples were gated on CD45<sup>+</sup> CD4<sup>+</sup> CD3<sup>+</sup> cells (*n*=6). MFI, mean fluorescence intensity

discovery set and MIBC patients receiving ACT are relatively small. Second, serial surgical sections were used for immunostaining CD19, MHC II, and CD4, so the results

cannot reflect the precise positioning of cells. Therefore, a prospective, randomized, larger population trial is needed to validate these results in the future. Overall, our study found

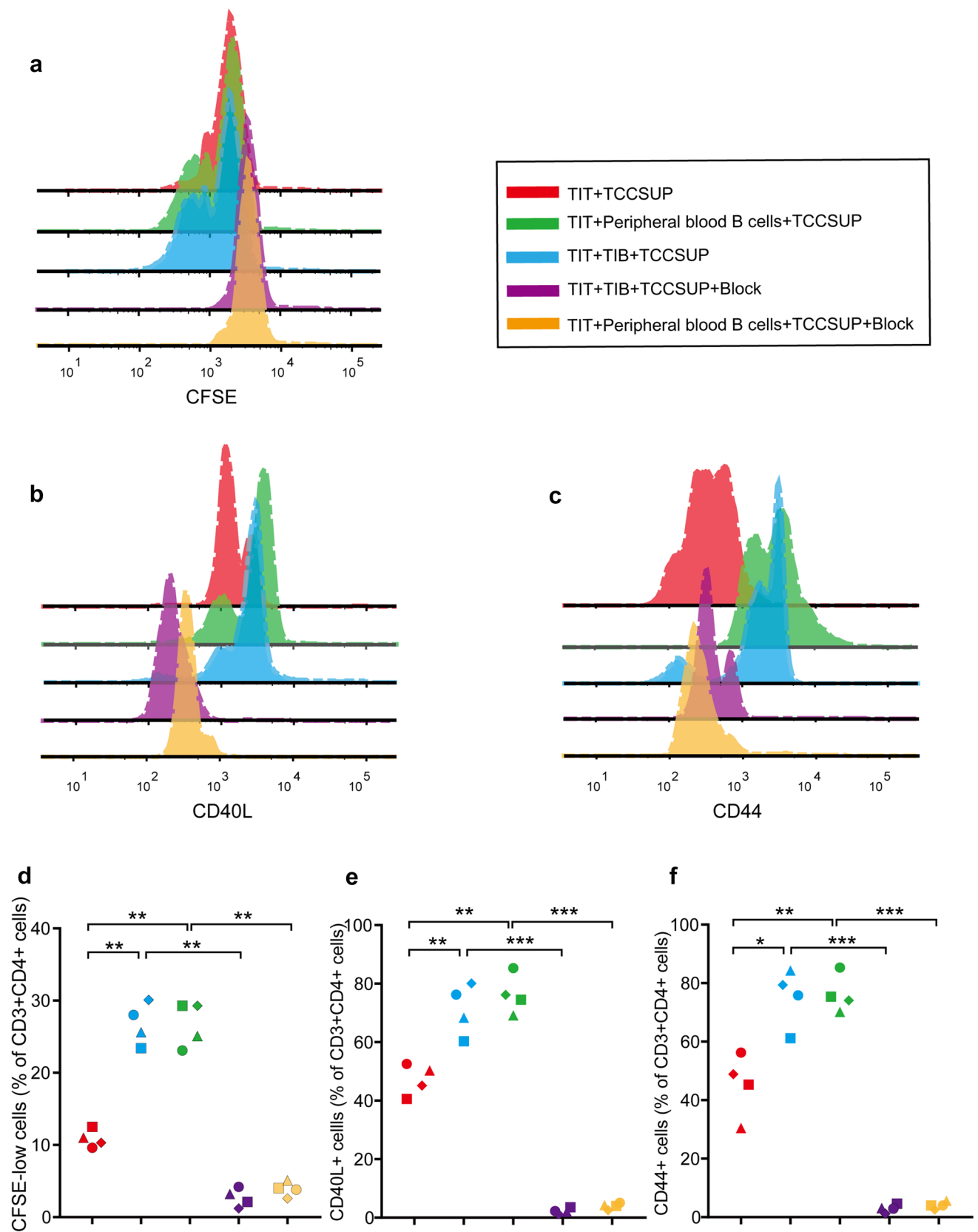


**Fig. 5** Ag presentation assay of CD19<sup>+</sup>TIB. **a–c** Representative FACS histogram showing CFSE dilution, expression of CD44 and CD40L on CD4<sup>+</sup> TIT when: CFSE-labeled CD4<sup>+</sup> TIT were cocultured with TCCSUP lysates (red), labeled CD4<sup>+</sup> TIT were cocultured with peripheral blood B-cells and TCCSUP lysates (green), labeled CD4<sup>+</sup> TIT were cocultured with CD19<sup>+</sup> TIB and TCCSUP lysates (blue), labeled CD4<sup>+</sup> TIT were cocultured with CD19<sup>+</sup> TIB and TCCSUP lysates and HLA-DR blocking antibodies (purple), labeled CD4<sup>+</sup> TIT were cocultured with peripheral blood B-cells and TCCSUP lysates and HLA-DR blocking antibodies (orange). **d–f** CFSE<sup>+</sup> CD4<sup>+</sup> T-cell, CD40L<sup>+</sup> CD4<sup>+</sup> T-cell and CD44<sup>+</sup> CD4<sup>+</sup> T-cell frequencies in MIBC ( $n=4$ ). \* $P<0.05$ , \*\* $P<0.01$ , \*\*\* $P<0.001$

a superior treatment effect of platinum-based ACT in high CD19<sup>+</sup> TIB MIBC patients, which could be explained by the enhanced antigen-presentation capacity of activated CD19<sup>+</sup> TIB in MIBC patients. In the future, these results could aid clinical decision-making concerning platinum-based chemotherapy in high CD19<sup>+</sup> TIB MIBC patients after cystectomy and routine pathological assessment.

## Conclusions

In conclusion, our study identified that MIBC patients with high CD19<sup>+</sup> TIB had better survival and might benefit more from platinum-based ACT; CD19<sup>+</sup> TIB can be used as a novel independent predictor for post-surgery prognosis in MIBC. In vitro coculture experiments suggest that CD19<sup>+</sup> B-cells may serve as APCs to activate CD4<sup>+</sup> TIT in the tumor environment of MIBC.

**Author contributions** QJ, QF and YC: acquisition of data, analysis and interpretation of data, statistical analysis and drafting the manuscript. ZL, JZ, LX, YZ and YW: technical and material support. WZ and JX: study concept and design, analysis and interpretation of data, drafting the manuscript, obtained the funding and study supervision. All authors read and approved the final manuscript.

**Funding** This study was funded by grants from the National Natural Science Foundation of China (81471621, 81472227, 81671628, 31770851, 81871306 and 81872082), the Shanghai Municipal Natural Science Foundation (17ZR1405100), the Shanghai Sailing Program (18YF1404500) and the Shanghai Municipal Commission of Health and Family Planning Program (20144Y0223). The study sponsors had no roles in the study design or in the collection, analysis, and interpretation of data.

## Compliance with ethical standards

**Conflict of interest** The authors declare no conflict of interest.

**Ethical approval and ethical standards** This study was approved by the institutional ethical review boards of Zhongshan Hospital, Fudan University (Registration no. B2015-030) and Fudan University Shanghai Cancer Center (Registration no. 050432-4-1212B). Written informed consent approved by the institutional ethics committee was obtained from each patient.

## References

- Siegel RL, Miller KD, Jemal A (2017) Cancer statistics, 2017. *CA Cancer J Clin* 67:7–30. <https://doi.org/10.3322/caac.21387>
- Bellmunt J, Orsola A, Leow JJ, Wiegel T, De Santis M, Horwich A, Group EGW (2014) Bladder cancer: ESMO practice guidelines for diagnosis, treatment and follow-up. *Ann Oncol* 25 Suppl 3: iii40–i8. <https://doi.org/10.1093/annonc/mdu223>
- Witjes JA, Comperat E, Cowan NC et al (2014) EAU guidelines on muscle-invasive and metastatic bladder cancer: summary of the 2013 guidelines. *Eur Urol* 65:778–792. <https://doi.org/10.1016/j.eururo.2013.11.046>
- Alfred Witjes J, Lebret T, Comperat EM et al (2017) Updated 2016 EAU guidelines on muscle-invasive and metastatic bladder cancer. *Eur Urol* 71:462–475. <https://doi.org/10.1016/j.eururo.2016.06.020>
- Pylayeva-Gupta Y, Das S, Handler JS, Hajdu CH, Coffre M, Koralov SB, Bar-Sagi D (2016) IL35-producing B cells promote the development of pancreatic neoplasia. *Cancer Discov* 6:247–255. <https://doi.org/10.1158/2159-8290.CD-15-0843>
- Shalpour S, Lin XJ, Bastian IN et al (2017) Inflammation-induced IgA<sup>+</sup> cells dismantle anti-liver cancer immunity. *Nature* 551:340–345. <https://doi.org/10.1038/nature24302>
- Cooper MD (2015) The early history of B cells. *Nat Rev Immunol* 15:191–197. <https://doi.org/10.1038/nri3801>
- Vidard L, Kovacsovic-Bankowski M, Kraeft SK, Chen LB, Benacerraf B, Rock KL (1996) Analysis of MHC class II presentation of particulate antigens of B lymphocytes. *J Immunol* 156:2809–2818
- Senovilla L, Vacchelli E, Galon J et al (2012) Trial watch: prognostic and predictive value of the immune infiltrate in cancer. *Oncoimmunology* 1:1323–1343. <https://doi.org/10.4161/onci.22009>
- Inoue S, Leitner WW, Golding B, Scott D (2006) Inhibitory effects of B cells on antitumor immunity. *Cancer Res* 66:7741–7747. <https://doi.org/10.1158/0008-5472.CAN-05-3766>
- Schioppa T, Moore R, Thompson RG, Rosser EC, Kulbe H, Nedospasov S, Mauri C, Coussens LM, Balkwill FR (2011) B regulatory cells and the tumor-promoting actions of TNF-alpha during squamous carcinogenesis. *Proc Natl Acad Sci U S A* 108:10662–10667. <https://doi.org/10.1073/pnas.1100994108>
- Montfort A, Pearce O, Maniati E et al (2017) A strong B-cell response is part of the immune landscape in human high-grade serous ovarian metastases. *Clin Cancer Res* 23:250–262. <https://doi.org/10.1158/1078-0432.Ccr-16-0081>
- Cerami E, Gao J, Dogrusoz U et al (2012) The cBio cancer genomics portal: an open platform for exploring multidimensional cancer genomics data. *Cancer Discov* 2:401–404. <https://doi.org/10.1158/2159-8290.CD-12-0095>
- Zhang L, Conejo-Garcia JR, Katsaros D et al (2003) Intratumoral T cells, recurrence, and survival in epithelial ovarian cancer. *N Engl J Med* 348:203–213. <https://doi.org/10.1056/NEJMoa020177>
- Ke AW, Shi GM, Zhou J et al (2009) Role of overexpression of CD151 and/or c-met in predicting prognosis of hepatocellular carcinoma. *Hepatology* 49:491–503. <https://doi.org/10.1002/hep.22639>
- Subramanian A, Tamayo P, Mootha VK et al (2005) Gene set enrichment analysis: a knowledge-based approach for interpreting genome-wide expression profiles. *Proc Natl Acad Sci U S A* 102:15545–15550. <https://doi.org/10.1073/pnas.0506580102>
- Newman AM, Liu CL, Green MR, Gentles AJ, Feng W, Xu Y, Hoang CD, Diehn M, Alizadeh AA (2015) Robust enumeration of cell subsets from tissue expression profiles. *Nat Methods* 12:453–457. <https://doi.org/10.1038/nmeth.3337>

18. Murphy K, Weaver C (2016) *Janeway's immunobiology*. Garland Science, London. ISBN-13: 978-0-8153-4551-0
19. Qu Y, Chen L, Lowe DB, Storkus WJ, Taylor JL (2012) Combined Tbet and IL12 gene therapy elicits and recruits superior antitumor immunity in vivo. *Mol Ther* 20:644–651. <https://doi.org/10.1038/mt.2011.283>
20. Davis RE, Ngo VN, Lenz G et al (2010) Chronic active B-cell-receptor signalling in diffuse large B-cell lymphoma. *Nature* 463:88–97. <https://doi.org/10.1038/nature08638>
21. Siddik ZH (2003) Cisplatin: mode of cytotoxic action and molecular basis of resistance. *Oncogene* 22:7265–7279. <https://doi.org/10.1038/sj.onc.1206933>
22. Leow JJ, Martin-Doyle W, Rajagopal PS et al (2014) Adjuvant chemotherapy for invasive bladder cancer: a 2013 updated systematic review and meta-analysis of randomized trials. *Eur Urol* 66:42–54. <https://doi.org/10.1016/j.eururo.2013.08.033>
23. Choi W, Porten S, Kim S et al (2014) Identification of distinct basal and luminal subtypes of muscle-invasive bladder cancer with different sensitivities to frontline chemotherapy. *Cancer Cell* 25:152–165. <https://doi.org/10.1016/j.ccr.2014.01.009>
24. Fremd C, Schuetz F, Sohn C, Beckhove P, Domschke C (2013) B cell-regulated immune responses in tumor models and cancer patients. *Oncoimmunology* 2:e25443. <https://doi.org/10.4161/onci.25443>
25. Shi JY, Gao Q, Wang ZC et al (2013) Margin-infiltrating CD20(+) B cells display an atypical memory phenotype and correlate with favorable prognosis in hepatocellular carcinoma. *Clin Cancer Res* 19:5994–6005. <https://doi.org/10.1158/1078-0432.CCR-12-3497>
26. DiLillo DJ, Yanaba K, Tedder TF (2010) B cells are required for optimal CD4 + and CD8 + T cell tumor immunity: therapeutic B cell depletion enhances B16 melanoma growth in mice. *J Immunol* 184:4006–4016. <https://doi.org/10.4049/jimmunol.0903009>
27. Apetoh L, Ghiringhelli F, Tesniere A et al (2007) Toll-like receptor 4-dependent contribution of the immune system to anticancer chemotherapy and radiotherapy. *Nat Med* 13:1050–1059. <https://doi.org/10.1038/nm1622>
28. Wang W, Kryczek I, Dostal L et al (2016) Effector T cells abrogate stroma-mediated chemoresistance in ovarian cancer. *Cell* 165:1092–1105. <https://doi.org/10.1016/j.cell.2016.04.009>